

Ultra-fast x-ray-dynamic experimental subsystem

Liming Chen(陈黎明), Xin Lu(鲁欣), Dazhang Li(李大章), Yifei Li(李毅飞)

Citation: Chin. Phys. B . 2018, 27(7): 074101. **doi:** 10.1088/1674-1056/27/7/074101

Journal homepage: http://cpb.iphy.ac.cn; http://iopscience.iop.org/cpb

What follows is a list of articles you may be interested in

Dynamic study of compressed electron layer driven by linearly polarized laser

Feng-chao Wang(王凤超)

Chin. Phys. B . 2016, 25(5): 054102. **doi:** 10.1088/1674-1056/25/5/054102

Numerical simulation for all-optical Thomson scattering X-ray source

Tan Fang, Zhu Bin, Han Dan, Xin Jian-Ting, Zhao Zong-Qing, Cao Lei-Feng, Gu Yu-Qiu, Zhang Bao-Han

Chin. Phys. B . 2014, 23(3): 034104. **doi:** 10.1088/1674-1056/23/3/034104

Effects of density profile and multi-species target on laser-heated thermal-pressure-driven shock wave acceleration

Wang Feng-Chao

Chin. Phys. B . 2013, 22(12): 124102. **doi:** 10.1088/1674-1056/22/12/124102

Electron acceleration by tightly focused radially polarized few-cycle laser pulses

Liu Jin-Lu,Sheng Zheng-Ming,Zheng Jun

Chin. Phys. B . 2012, 21(2): 024101. **doi:** 10.1088/1674-1056/21/2/024101

TOPICAL REVIEW — Synergetic Extreme Condition User Facility: Breakthroughs and opportunities for the research of physical science

Ultra-fast x-ray-dynamic experimental subsystem*

Liming Chen(陈黎明)[1,2,†], Xin Lu(鲁欣)[1,2], Dazhang Li(李大章)[1], and Yifei Li(李毅飞)[1]

[1] *Beijing National Laboratory of Condensed Matter Physics, Institute of Physics, Chinese Academy of Sciences, Beijing* 100190, *China*
[2] *School of Physical Sciences, University of Chinese Academy of Science, Beijing* 100190, *China*

(Received 27 April 2018; revised manuscript received 24 May 2018; published online 1 June 2018)

Ultra-fast x-ray-dynamic experimental subsystem is a facility which can provide femtosecond hard x-ray sources using a femtosecond laser interacting with plasmas. By utilizing these ultra-fast x-rays as a probe, combined with a naturally synchronized driver laser as a pump, we can perform dynamic studies on samples with a femtosecond time resolution. This subsystem with a four-dimensional ultra-high spatiotemporal resolution is a powerful tool for studies of the process of photosynthesis, Auger electron effects, lattice vibrations, etc. Compared with conventional x-ray sources based on accelerators, this table-top laser-driven x-ray source has significant advantages in terms of the source size, pulse duration, brightness, flexibility, and economy. It is an effective supplement to the synchrotron light source in the ultrafast detection regime.

Keywords: ultra-fast x-ray diffraction/absorption, time-resolved pump–probe detection, ultra-high-spatiotemporal-resolution detection

PACS: 41.75.Jv, 01.52.+r, 01.50.Pa, 94.05.Rx **DOI:** 10.1088/1674-1056/27/7/074101

1. Introduction

X-ray emission has been one of the most effective methods to investigate the properties of matter in various scientific fields.[1] In the accelerator community, synchrotron light sources have been useful for a broad range of users, in particular, in biological and condensed-matter applications.[2] Moreover, x-ray free-electron laser (XFEL) facilities have been recently constructed and started to operate,[3] which are expected to have revolutionary impacts on science and technology. However, they are inappropriate for some applications owing to the high cost, large experimental footprint, relatively long pulse structure, and poly-chromaticity. Owing to the rapid progress of the femtosecond laser technology, the ultra-fast hard-x-ray emissions from femtosecond-(fs)-laser-produced plasmas have been extensively studied over the past years,[4–6] including the K_α x-ray source,[7–9] betatron radiation,[10,11] inverse Compton scattering,[12,13] and high-harmonic generation.[14] Among them, the K_α x-ray sources have been extensively investigated; their source energy conversion efficiencies and temporal durations have been significantly improved.[6–8,15–17]

These ultra-short ultra-small laser-produced K_α x-ray sources can provide an alternative to accelerator-based light sources owing to their compactness and high brightness, making them practical for widespread applications in fundamental science, industry, and medicine.[18–20] Compared to x-ray tubes, they have the advantages of ultra-fast characteristic and high brightness. Moreover, a very important advantage of the laser-driven x-ray source is the precise natural synchronization between the laser and generated x-rays. In time-resolved pump–probe experiments, the pump laser and probe x-ray originate from the same laser beam. Therefore, this would be very suitable and convenient for time-resolved x-ray pump–probe studies,[20,21] such as time-resolved x-ray diffraction[22–28] and x-ray absorption.[21,29] The size of the laser-driven K_α source is determined by the laser focal spot size, which is at the microscale; therefore, the laser-driven K_α source size is also at the microscale. These micro-x-ray-sources are of significance in phase contrast imaging for the development of high-resolution diagnostics in biology[30,31] and medicine.[32]

In this paper, we present our preliminary design for an ultra-fast x-ray-dynamic subsystem, which can provide hard femtosecond x-ray radiation in both 100-Hz and single-shot modes. The schematic of this subsystem is shown in Fig. 1. The femtosecond laser pulse is split into two beams by a beam splitter. One laser beam is used to pump the sample to induce an excitation, while the other one is focused and interacted with the solid or cluster target to produce ultra-fast x-rays. The generated x-rays are collected and focused on the sample for studies using x-ray diffraction, imaging, and absorption spectroscopy. The samples exhibit dynamic changes after the pumping. Therefore, by changing the time delay between the pump laser and x-rays, the samples' transient structures and ultra-fast-dynamic information can be obtained.

*Project supported by the National Major Science and Technology Infrastructure Construction Project "Synergetic Extreme Condition User Facility", China.
†Corresponding author. E-mail: lmchen@iphy.ac.cn
© 2018 Chinese Physical Society and IOP Publishing Ltd

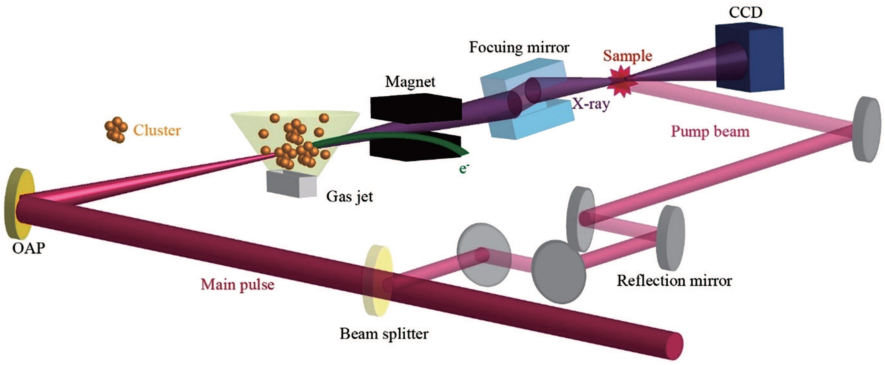


Fig. 1. (color online) Principle of ultra-fast x-ray dynamic subsystem.

The rest of this paper is organized as follows. In Section 2, we briefly introduce the subsystem. In Sections 3–5, we introduce the main units of the system and their functions. In the last section, a short summary is presented.

2. Overall system and functional units

The overall design of this subsystem is shown in Fig. 2. The facility has eight main functional units: ultra-intense femtosecond laser unit, optical transmission unit, x-ray source chamber unit, user application chamber unit, beam positioning unit, vacuum equipment unit, optical platform, and target chamber support unit. Among these units, the ultra-intense femtosecond laser, x-ray source, and user target chamber units are the most important. The ultra-intense laser pulse is output from the laser unit and guided to the target chamber unit through the optical transmission, beam position, and optical/chamber support units. In the target chamber, it interacts with solid/gas/cluster targets and produces hard x-rays. These xrays are focused onto the user application chamber unit for sample detection applications. We present a detailed description of these three parts in the following sections.

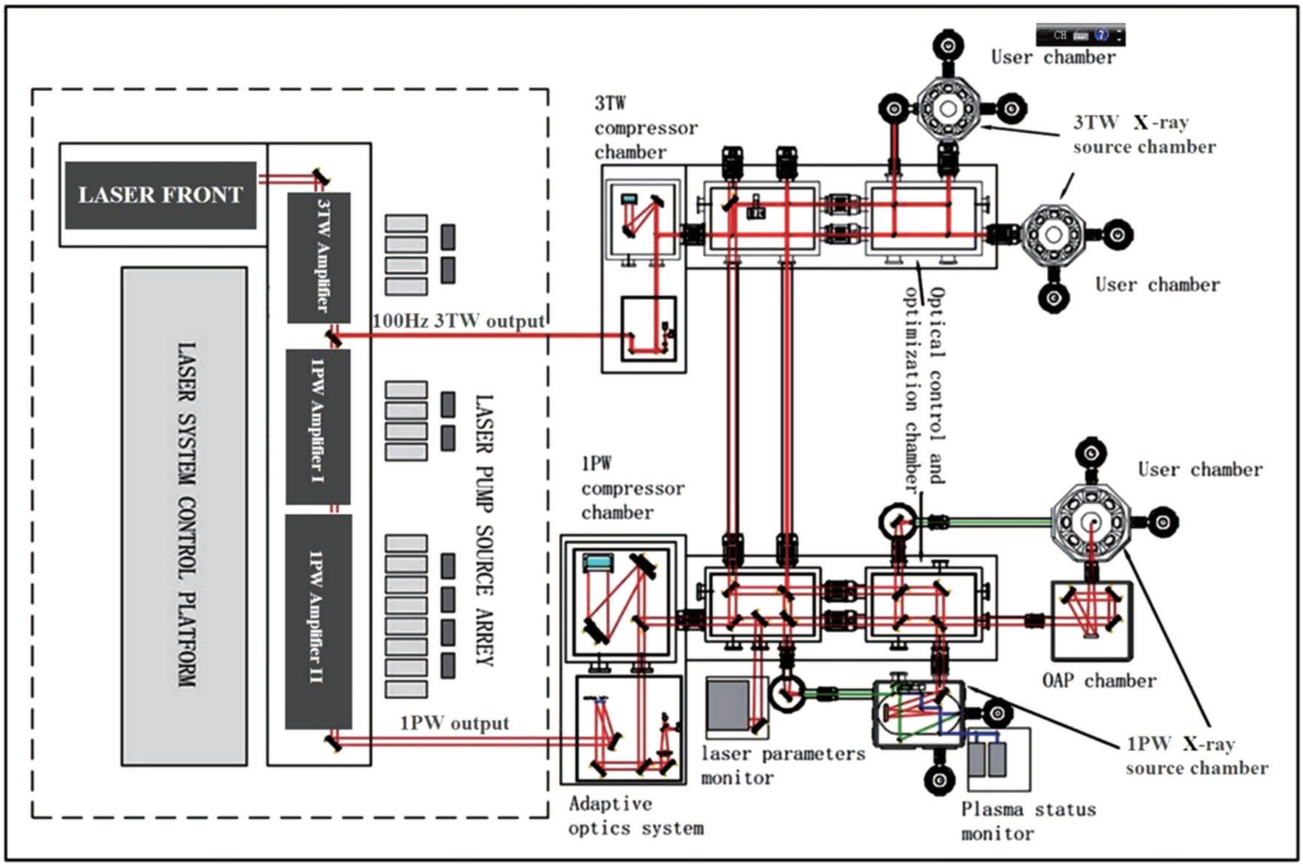


Fig. 2. (color online) Schematic setup of the ultrafast x-ray dynamics experimental subsystem.

3. Ultra-intense femtosecond laser unit

The ultra-intense femtosecond laser system consists of a front end (oscillator, stretcher, and kilohertz regenerative amplifier), a 100 Hz amplifier, a 10 Hz preamplifier, a main amplifier, and two compression chambers. The laser system can provide a two-stage ultra-fast and ultra-intense output, corresponding to different x-ray beam modes; the parameters of the first stage are 100 Hz, 3-TW output, and it is used for the x-ray beam line with a high-repetition-rate mode, which can generate x-rays with photon energies of 1–60 keV, photon number of 10^8/shot, and pulse duration smaller than 1 ps at a repetition rate of 100 Hz; the parameters for the second stage are 0.017 Hz, 1-PW output, and it is used for the intense x-ray beam line with a single-shot mode, which can deliver x-rays with photon energies of 3–20 keV, photon number of 10^{11}/shot, and pulse duration smaller than 1 ps. Specific technical parameters are listed in Table 1.

Table 1. Specific laser technical parameters.

	Wavelength /nm	Pulse duration/fs	Energy stability	Beam quality	Pointing stability	Polarization ratio	Contrast				
							pelica	ASE@1 ps	ASE@5 ps	ASE@50 ps	ASE@300 ps
100 Hz 3 TW	800	17	$< 2\% < 4\%$ 1 hour 1 day	$M^2 < 1.2$	< 20 rad	$< 1:100$	$> 10^8$	$> 10^3$	$> 10^5$	$> 10^9$	$> 10^{10}$
1 PW	800	25	$< 2\% < 5\%$ 0.5 hour 1 day	$M^2 < 1.5$	< 30 rad	$< 1:100$	$> 10^8$				

4. X-ray source unit

The two-stage laser beams are compressed into ultrashort laser pulses through their compression chambers, and then enter the solid or cluster target chamber through the optical transmission unit. Once focused, the laser beam interacts with the target to generate intense ultra-fast x-ray pulses. For different applications, three different types of target chambers are proposed: solid-target chamber, small-focal-length cluster-target chamber, and large-focal-length gas/clustertarget chamber. The x-ray fluxes from these three target chambers are different; therefore, the chamber structures and corresponding diagnostic tools are also different. We will introduce them in the following sections.

4.1. Solid-target chamber

The layout of the solid-target chamber is shown in Fig. 3. The 100-Hz main laser is focused on the surface of the disk-shaped solid target by a small-focal-length OAP to generate x-ray radiation. The disk target is mounted on a multi-dimensional motorized stage, which can rotate around its axis. The target's surface roughness is better than 2 μm. An imaging charge-coupled device (CCD) used to monitor the target surface is installed outside the target chamber. The x-rays generated by the target are collected, collimated, and focused before they enter the user target chamber. The material of the disk-shaped solid target can be metals such as Cu, Ag, Mo, Ta, etc. to generate K_α radiations with different photon energies.

4.2. Small-focal-length cluster-target chamber

The layout is shown in Fig. 4. The main laser beam is focused by a small-focal-length OAP (the focal length is 500 mm) on the clustering gas from a supersonic gas nozzle to generate x-rays. A low-energy laser beam separated from the main laser is divided into two parts. One of them acts as a pump beam to irradiate the sample to stimulate the ultra-fast process, while the other one acts as a probe beam, which passes through the clustered plasmas. It can be employed for

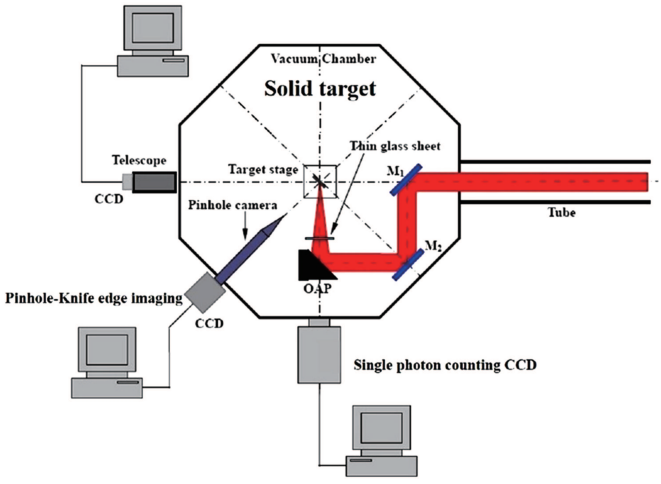


Fig. 3. (color online) Schematic of the solid target chamber.

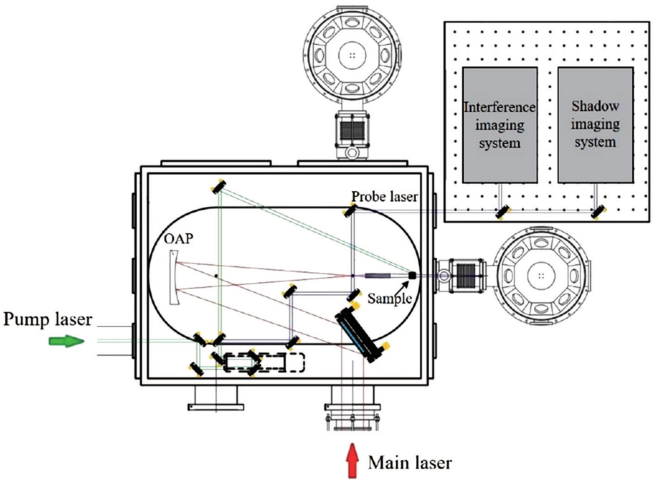


Fig. 4. (color online) Schematic setup of the short focal cluster target chamber.

shadow imaging and interference analysis, which can be used to obtain plasma distribution and evolution information. The small-focal-length cluster-target chamber is characterized by a relatively small x-ray source size, which is more suitable for single-shot x-ray imaging applications.

4.3. Large-focal-length cluster-target chamber

The layout is shown in Fig. 5. The main laser enters a special chamber for the installation of the large-focal-length OAP (focal length: 1500 mm), where the laser is focused through a vacuum tube into the interaction target chamber. The pump and probe beams are similar with those at the small-focal-length condition. The large-focal-length cluster/gastarget chamber is characterized by a high x-ray flux in a single laser shot, which is more suitable for single-shot x-ray diffraction and absorption spectroscopy.

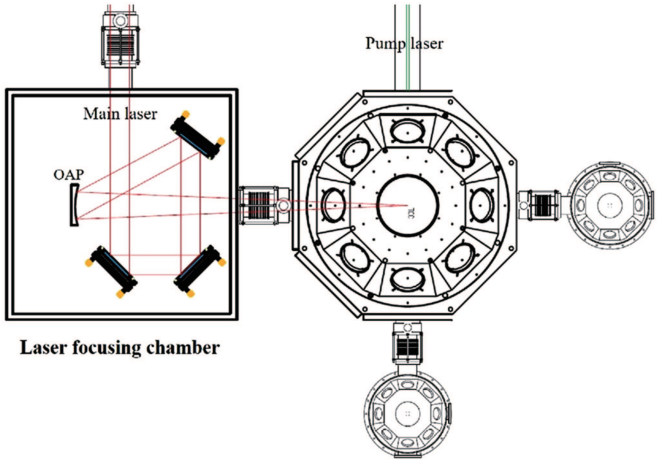


Fig. 5. (color online) Schematic setup of the long-focal-length cluster-target chamber.

4.4. X-ray source specification

The x-ray source parameters are measured by various diagnostic equipments installed around the target chamber, including x-ray pinhole imaging CCD and single-photon counting CCD, as shown in Fig. 3. The pinhole imaging CCD is used to measure the x-ray source size. The single-photon counting CCD is used to analyze the x-ray energy spectrum and intensity. The diagnostic equipment has a similar design for the cluster-target chamber. The x-ray sources in the above three chambers can be divided into two categories.

Ultra-fast x-ray source I (solid target) Photon energy: 1–60 keV (discrete spectral lines can be achieved by changing the target material), time width: < 1 ps, source size: 2–100 μm, photon number: 10^8/shot, stability: better than 10%, repetition rate: 100 Hz.

Ultra-fast x-ray source II (cluster target) Photon energy: 3–20 keV (discrete spectral lines can be achieved by changing the target material), time width: < 1 ps, source size: 5–100 μm, photon number: 10^{11}/shot.

5. User target chamber unit

The x-ray user unit is mainly composed of a sample holder with four-dimensional (4D) adjusting stages, a Montel x-ray reflective focusing mirror, x-ray imaging devices, x-ray absorption spectroscopy devices, and x-ray diffraction devices. The x-rays generated from the laser–target interaction are mainly from the inner shell and Bremsstrahlung radiations, with 4π distributions, and intensities inversely proportional to the square of the distance. In order to increase the x-ray intensity on the sample, the x-rays are collected, collimated, and focused by the Montel x-ray reflective focusing lens. Between the x-ray source and x-ray optics, a strong magnet is employed to deflect the produced high-energy electrons, so that they do not interfere with the analysis. In the following sections, we introduce the design of the user chamber for three applications: x-ray imaging, absorption, and diffraction spectroscopy.

5.1. Ultra-fast x-ray imaging system

As x-rays pass through a sample, materials with different densities and thicknesses have different x-ray attenuation rates and phase changes. Therefore, one can obtain the sample's two-dimensional structure by collecting the transmitted x-ray signals. The layout of the ultra-fast x-ray imaging diagnostics is shown in Fig. 6(a). The x-ray beam is collected and focused by the Montel-type reflective focusing lens, and then irradiates the sample. The transmitted x-rays are converted into visible light on the phosphor screen, and finally recorded by the CCD with a large array. If the x-ray source is sufficiently strong and has a small size, the focusing system may not be used. The combination of the phosphor screen and CCD can be replaced by an imaging plate (IP). Our team has extensive experience on using laser-generated ultra-fast x-rays for imaging. We achieved single-shot monochromatic imaging using a K-shell x-ray source with a cluster target in 2010.[8] Figures 6(b) and 6(c) show the experimental K_α x-ray spectrum[8] and x-ray image of a cicada wing.[33]

5.2. Ultra-fast x-ray absorption spectroscopy system

The layout of the ultra-fast x-ray absorption spectroscopy system is shown in Fig. 7. The absorption spectroscopy mainly uses bremsstrahlung x-rays generated from the interaction between the laser and high-Z material. The x-ray beam passes through the sample and then enters the NIST transmission crystal spectrometer for an absorption-spectrum measurement. It can also perform time-resolved absorption spectroscopy by introducing the pump laser. A test sample is mounted on a multi-dimensional holder (three-dimensional translation stages and one-dimensional rotation stage). As shown in Ref. [21], typical experimental near-edge x-ray absorption fine structure (NEXAFS) and/or extended x-ray absorption near-edge spectra (iron K edge) can be obtained from Fe(III) oxalate after transformation to μX vs. E at -20 ps before excitation and $+25$ ps after excitation; the solid/dotted lines represent different pump delays.

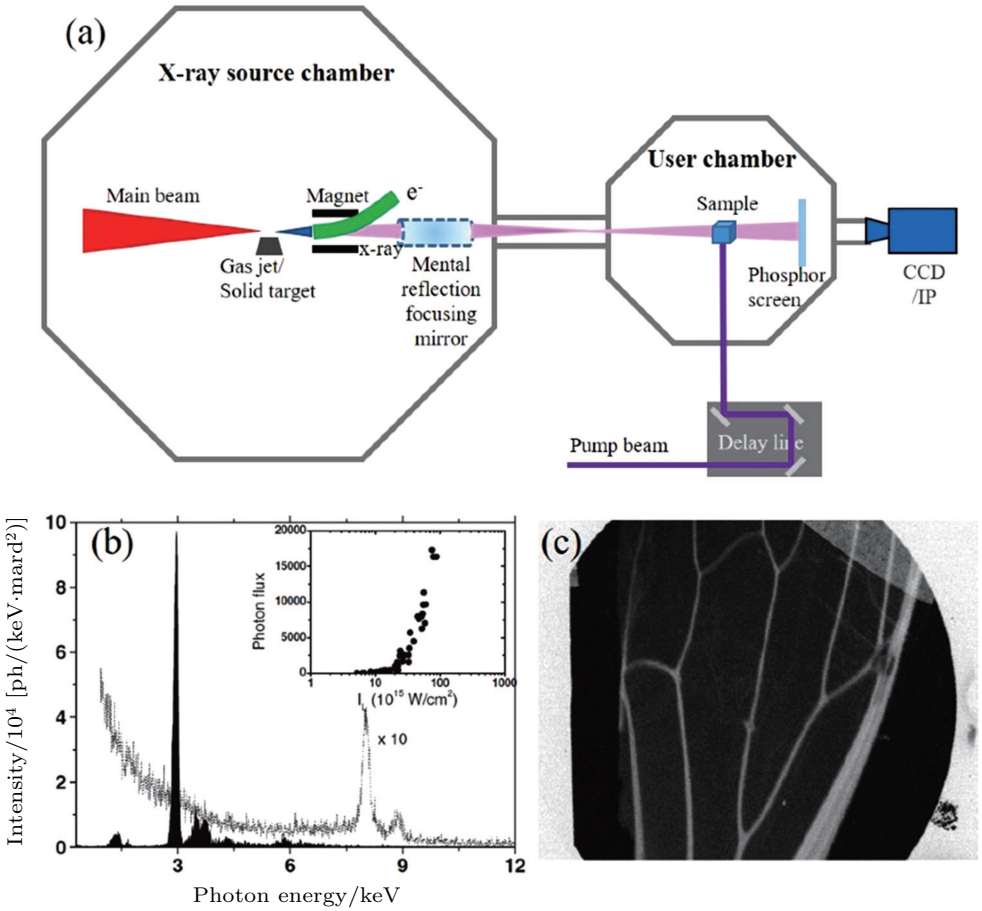


Fig. 6. (color online) (a) Schematic of ultrafast x-ray imaging system. (b) X-ray spectrum of K_α, the black line shows Ar cluster target's result, the grey dotted line shows a solid Cu target's result with $\times 10$ in amplitude, and the inset is the photon flux dependence on laser intensity.[8] (c) Single shot x-ray image of cicada wing.[33]

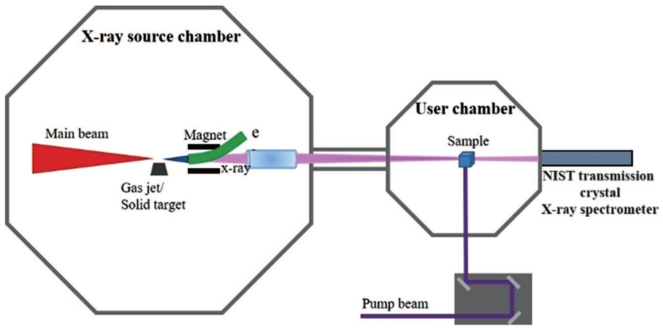


Fig. 7. (color online) Schematic of ultrafast x-ray absorption spectroscopy system.

5.3. Ultra-fast x-ray diffraction system

Ultra-fast x-ray diffraction can be performed in the transmitted or reflective mode; the layouts of these modes are shown in Figs. 8(a) and 8(b), respectively.

The x-rays are focused on the sample by a Montel x-ray reflective focusing lens, and then diffract. The transmitted diffracted light forms a diffraction pattern on the phosphor screen, recorded by the large-array CCD. Transmitted x-ray diffraction is only applicable to thin samples. For thicker samples, reflective x-ray diffraction can be used to study the ultrafast dynamics of its surface. In the reflective diffraction mode, the x-rays irradiate the sample surface. The diffraction fringes of the x-rays can be observed in the reflection direction, as shown in Fig. 8(c).

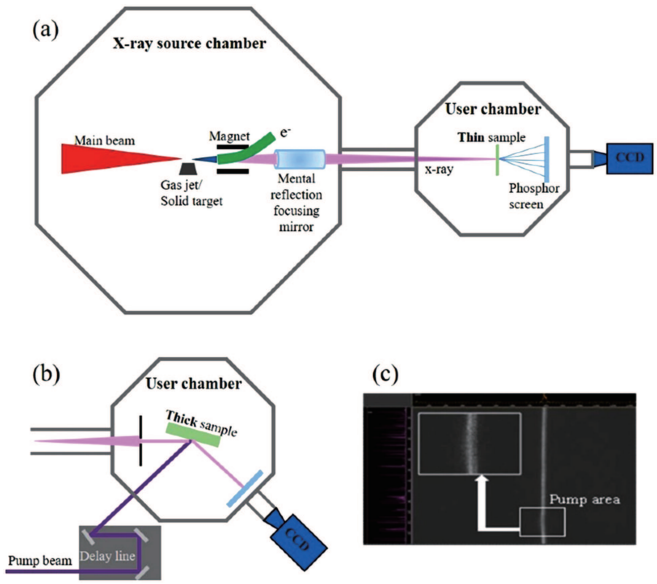


Fig. 8. (color online) (a) Schematic of transmitted x-ray diffraction system. (b) Schematic of reflective x-ray diffraction system. (c) The diffracted signal from the 200-nm Au (111) crystal.

6. Summary

We introduced here the ultra-fast x-ray-dynamic experimental subsystem. Details of the design of the main units were presented. With this facility, we expect to provide two types of stable x-ray sources to scientific users: 100 Hz mode with 10^8 photons/shot and photon energy of 1–60 keV, and single-shot mode with 10^{11} photons/shot and photon energy of 3–20 keV. The whole proposal is technically feasible according to our experimental results in the past several years.

This ultra-fast ultra-intense x-ray-dynamic subsystem involves two main innovations. First, in the 100 Hz mode, for the first time, a laser-driven second-generation high-quality ultra-fast x-ray source is used for a 4D-spatiotemporal-resolution detection of ultra-fast dynamic processes. Compared with the first-generation laser-plasma-based sources widely used in other laboratories, the developed quality-improved x-ray source of the presented subsystem significantly improves the conversion efficiency, source size, and signal-to-noise ratio, leading to a significantly higher imaging quality. Second, in the single-shot mode with a high power laser, single-shot x-ray time-resolved imaging and diffraction can be performed for the first time for various applications, separating the high-power laser pulse to 10 sub-pulses to drive individual x-ray beams for imaging. The spatiotemporal diagnosis with a single laser pulse, which can be applied to a single irreversible ultra-fast process with random characteristics, is of significance in biophysics, high-pressure physics, and high-energy-density physics.

Acknowledgment

We thank the colleagues of high energy density physics group in Laboratory of Optical Physics, Institute of Physics and Chinese Academy of Sciences for the help and support.

References

[1] Corde S, Ta Phuoc K, Lambert G, Fitour R, Malka V, Rousse A, Beck A and Lefebvre E 2013 *Rev. Mod. Phys.* **85** 1
[2] Sinha S K, Glyde H, Briber R and Takata M 2010 *Synchrotron Radiat. News* **23** 33
[3] Emma P, Akre R, Arthur J, Bionta R, Bostedt C, Bozek J, Brachmann A, Bucksbaum P, Coffee R, Decker F J, Ding Y, Dowell D, Edstrom S, Fisher A, Frisch J, Gilevich S, Hastings J, Hays G, Hering P, Huang Z, Iverson R, Loos H, Messerschmidt M, Miahnahri A, Moeller S, Nuhn H D, Pile G, Ratner D, Rzepiela J, Schultz D, Smith T, Stefan P, Tompkins H, Turner J, Welch J, White W, Wu J, Yocky G and Galayda J 2010 *Nat. Photon.* **4** 641
[4] Corde S, Ta K, Lambert G, Fitour R, Malka V and Rouse A 2013 *Rev. Mod. Phys.* **85** 1
[5] Albert F and Thomas Alec G R 2014 *Plasma Phys. Control. Fusion* **56** 103001
[6] Teubner U and Gibbon P 2009 *Rev. Mod. Phys.* **81** 445
[7] Kieffer J C, Krol A, Jiang Z, Chamberlain C C, Scalzetti E and Ichalalene Z 2002 *Appl. Phys. B* **74** s75
[8] Chen L M, Kando M, Xu M H, Li Y T, Koga J, Chen M, Xu H, Yuan X H, Dong Q L, Sheng Z M, Bulanov S V, Kato Y, Zhang J and Tajima T 2008 *Phys. Rev. Lett.* **100** 045004
[9] Chen L M, Liu F, Wang W M, Kando M, Mao J Y, Zhang L, Ma J L, Li Y T, Bulanov S V, Tajima T, Kato Y, Sheng Z M, Wei Z Y and Zhang J 2010 *Phys. Rev. Lett.* **104** 215004
[10] Kneip S, McGuffey C, Martins J L, Martins S F, Bellei C, Chvykov V, Dollar F, Fonseca R, Huntington C, Kalintchenko G, Maksimchuk A, Mangles S P D, Matsuoka T, Nagel S R, Palmer C A J, Schreiber J, Phuoc K T, Thomas A G R, Yanovsky V, Silva L O, Krushelnick K and Najmudin Z 2010 *Nat. Phys.* **6** 980
[11] Cipiccia S, Islam M R, Ersfeld B, Shanks R P, Brunetti E, Vieux G, Yang X, Issac R C, Wiggins S M, Welsh G H, Anania M P , Maneuski D, Montgomery R, Smith G, Hoek M, Hamilton D J, Lemos N R C, Symes D, Rajeev P P, Shea V O, Dias J M and Jaroszynski D A 2011 *Nat. Phys.* **7** 867
[12] Powers N D, Ghebregziabher I, Golovin G, Liu C, Chen S, Banerjee S, Zhang J and Umstadter D P 2014 *Nat Photon.* **8** 28
[13] Phuoc K T, Corde S, Thaury C, Malka V, Tafzi A, Goddet J P, Shah R C, Sebban S and Rousse S 2012 *Nat. Photon.* **6** 308
[14] Fleischer A, Kfir O, Diskin T, Sidorenko P and Cohen O 2012 *Nat. Phys.* **8** 108
[15] Murnane M M, Kapteyn H C, Rosen M D and Falcone R W 1991 *Science* **251** 531
[16] Rousse A, Audebert P, Geindre P, Fallies F, Gauthier J C, Mysyrowicz A, Grillon G and Antonetti A 1994 *Phys. Rev. E* **50** 2200
[17] Weisshaupt J, Juvé V, Holtz M, Ku S A, Woerner M, Elsaesser T, Ališauskas S, Pugžlys A and Baltuška A 2014 *Nat. Photon.* **8** 927
[18] Zewail A H 2000 *J. Phys. Chem. A* **104** 5660
[19] Bloembergen N 1999 *Rev. Mod. Phys.* **71** S283
[20] Rousse A, Rischel C and Gauthier J C 2001 *Rev. Mod. Phys.* **73** 17
[21] Er Ali Oguz, Chen J and Rentzepis Peter M 2012 *J. Appl. Phys.* **112** 031101
[22] Rousse A, Rischel C, Fourmaux S, Uschmann I, Sebban S, Grillon G, Balcou Ph, Förster E, Geindre J P, Audebert P, Gauthier J C and Hulin D 2001 *Nature* **410** 65
[23] Cavalleri A, Siders C W, Brown F L H, Leitner D M, Toth C, Squier J A, Barty C P J, Wilson K R, Sokolowski-Tinten K, Horn von Hoegen M, Linde D von der and Kammler D 2000 *Phys. Rev. Lett.* **85** 586
[24] Sokolowski-Tinten K, Blome C, Dietrich C, Tarasevitch A, Horn von Hoegen M, Linde D von der, Cavalleri A, Squier J and Kammler M 2001 *Phys. Rev. Lett.* **87** 225701
[25] Bargheer M, Zhavoronkov N, Gritsai Y, Woo J C, Kim D S, Woerner M and Elsaesser T 2004 *Science* **306** 1771
[26] Chen J, Chen W K, Tang J and Rentzepis P M 2011 *Proc. Natl. Acad. Sci. USA* **108** 18887
[27] Oguz Er A, Chen J, Tang J and Rentzepis P M 2012 *Appl. Phys. Lett.* **100** 151910
[28] Elsaesser T and Woerner M 2014 *J. Chem. Phys.* **140** 020901
[29] Dorchies F, Festa F, Recoules, Peyrusse O, Benuzzi-Mounaix A, Brambrink E, Levy A, Ravasio A, Koenig M, Hall T and Mazevet S 2015 *Phys. Rev. B* **92** 085117
[30] Toth R, Fourmaux S, Ozaki T, Servol M and Kieffer J C 2007 *Phys. Plasmas* **14** 053506
[31] Huang K, Li M H, Yan W C, Guo X, Li D Z, Chen Y P, Ma Y, Zhao J R, Li Y F, Zhang J and Chen L M 2014 *Rev. Sci. Instrum.* **85** 113304
[32] Krol A, Ikhlef A, Kieffer J C, Bassano D A, Chamberlain C C, Jiang Z, Pépin H and Prasad S C 1997 *Med. Physic* **24** 725
[33] Zhang L, Chen L M, Yuan D W, Yan W C, Wang Z H, Liu C, Shen Z W, Faenov A, Pikuz T, Skobelev I, Gasilov V, Boldarev A, Mao J Y, Li Y T, Dong Q L, Lu X, Ma J L, Wang W M, Sheng Z M and Zhang J 2011 *Opt. Express.* **19** 25812